

Bag model prediction for the nucleon's chiral-odd twist-3 distribution $h_L(x, Q^2)$ at high Q^2

Y. Kanazawa and Yuji Koike

Graduate School of Science and Technology, Niigata University, Ikarashi, Niigata 950-21, Japan

Abstract

We study the Q^2 evolution of the nucleon's chiral-odd twist-3 distribution $h_L(x, Q^2)$ starting from the MIT bag model calculation. A simple GLAP equation for $h_L(x, Q^2)$ obtained at large N_c is used for the Q^2 evolution. The correction due to the finite value of N_c is $O(1/N_c^2) \sim 10\%$ level. It turns out that the twist-3 contribution to $h_L(x, Q^2)$ is significantly reduced at $Q^2 = 10 \text{ GeV}^2$ in contrast to the $g_2(x, Q^2)$ case. This is due to the fact that the corresponding anomalous dimension for h_L is larger than that for g_2 at small n (spin).

arXiv:hep-ph/9703324v1 14 Mar 1997

The EMC measurement of the nucleon's g_1 structure function [1] inspired lots of theoretical activities on the nucleon's spin-structure functions in general as well as more precision measurements of g_1 [2]. These structure functions provide us with a rich source of information about the spin distributions of quarks and gluons inside the nucleon. Jaffe and Ji [3] discussed general features of the quark distributions of the nucleon and relevant places where they can be measured. The nucleon has three independent twist-2 quark distributions, $f_1(x, Q^2)$ (spin-average), $g_1(x, Q^2)$ (helicity asymmetry), $h_1(x, Q^2)$ (helicity flip), and three independent twist-3 quark distributions $e(x, Q^2)$, $g_2(x, Q^2)$, $h_L(x, Q^2)$. Twist-2 distributions have a simple parton model interpretation and contribute to various hard processes in the leading order with respect to $1/\sqrt{Q^2}$. (Q is the hard momentum of the external hard probe.) On the other hand, the twist-3 distributions represent complicated quark-gluon correlations in the nucleon, and is generally difficult to be measured, since they are often hidden behind the leading twist-2 contributions. However, g_2 and h_L can be measured in the absence of the leading twist-2 contributions through the proper asymmetries in the polarized deep inelastic scattering and the polarized Drell-Yan process, respectively [4, 3]. In this sense, they are interesting higher twist distribution functions. In fact, E143 collaboration [5] presented a first nonzero data for g_2 , which anticipates a forthcoming significant progress in twist-3 physics.

So far accumulated experimental data on f_1 and g_1 allowed us to parametrize in the next-to-leading order for f_1 [6] and for g_1 [7]. But nothing is known about the actual shape of h_1 , g_2 and h_L except some guess by the bag model calculations [3, 8, 9]. (Since there is no practical way of isolating e , it will not be considered in this work.) The bag model has been reasonably successful in describing various properties of hadrons [10], and has been applied to calculate the structure functions [8, 9, 11, 12, 13, 14]. Since the bag model is a low energy effective hadron model, its prediction for the structure functions has to be evolved to higher scale to confront experimental data. After the Q^2 evolution, it could approximately reproduce the valence parts of f_1 and g_1 . The purpose of this short note is to present the first and a rough estimate of the magnitude of $h_L(x, Q^2)$ at high Q^2 starting from the bag model calculation. We are especially interested in the speed of the Q^2 -evolution of h_L compared with that of g_2 and the chiral-odd twist-2 distribution h_1 . Since it is not our purpose here to construct a more realistic model, we shall not pursue the projection method to restore the translational invariance as was tried in [9, 12, 13, 14]. We refer those attempts to future studies.

We first recall the definition of the quark distributions in our interest [3]:

$$\int \frac{d\lambda}{2\pi} e^{i\lambda x} \langle PS | \bar{\psi}(0) \gamma_\mu \gamma_5 \psi(\lambda n) | Q | PS \rangle = 2 \left[g_1(x, Q^2) p_\mu (S \cdot n) + g_T(x, Q^2) S_{\perp\mu} + M^2 g_3(x, Q^2) S \cdot n n_\mu \right], \quad (1)$$

$$\int \frac{d\lambda}{2\pi} e^{i\lambda x} \langle PS | \bar{\psi}(0) \sigma_{\mu\nu} i \gamma_5 \psi(\lambda n) | Q | PS \rangle = 2 \left[h_1(x, Q^2) (S_{\perp\mu} p_\nu - S_{\perp\nu} p_\mu) / M + h_L(x, Q^2) M (p_\mu n_\nu - p_\nu n_\mu) (S \cdot n) + h_3(x, Q^2) M (S_{\perp\mu} n_\nu - S_{\perp\nu} n_\mu) \right], \quad (2)$$

where $|PS\rangle$ denotes the nucleon (mass M) state with the four momentum P and the spin S , and the two light-like vectors, p and n , are introduced by the relation $P^\mu = p^\mu + \frac{M^2}{2} n^\mu$, $p \cdot n = 1$, $p^2 = n^2 = 0$. For the nucleon moving in the z -direction, $p = \frac{P}{\sqrt{2}}(1, 0, 0, 1)$ and $n = \frac{1}{\sqrt{2}P}(1, 0, 0, -1)$. $P \rightarrow \infty$ corresponds to the infinite momentum frame and $\mathcal{P} = M/\sqrt{2}$

corresponds to the nucleon's rest frame. S^μ is decomposed as $S^\mu = (S \cdot n)p^\mu + (S \cdot p)n^\mu + S_\perp^\mu$. In (1) and (2), lightcone gauge, $n \cdot A \sim A^+ = 0$, was employed. The above distribution functions $g_{1,T}$ ($g_T = g_1 + g_2$) and $h_{1,L}$ etc are defined for each quark flavor $\psi = \psi^a$ ($a = u, d, s, \dots$) and have support $-1 < x < 1$ [15]. The replacement $\psi^a \rightarrow C\bar{\psi}^{aT}$, $\bar{\psi}^a \rightarrow -\psi^a C^{-1}$ defines the anti-quark distributions $g_{1,T}^{\bar{a}}(x)$ etc for each quark distribution $g_{1,T}^a(x)$ etc. They are related as $g_{1,T}^a(-x) = g_{1,T}^{\bar{a}}(x)$, $h_{1,L}^a(-x) = -h_{1,L}^{\bar{a}}(x)$. For the polarized deep inelastic scattering, physically measurable structure functions are the combination $\sum_a e_a^2(g_{1,T}^a(x) + g_{1,T}^{\bar{a}}(x))$ with the Bjorken x ($0 < x < 1$) and the electric charge of a (anti-)quark flavor a , e_a . Here and below, we often suppress the explicit Q^2 dependence of the distributions.

The Q^2 dependence of these structure functions is calculable in perturbative QCD. The twist-2 distributions, g_1 and h_1 , obey simple GLAP equations [16]. On the other hand, the Q^2 dependence of the twist-3 distributions, g_2 and h_L , is quite sophisticated because the number of quark-gluon-quark operators increases with the moments (or spin). The calculation of the one-loop anomalous dimension matrix for all the twist-3 distributions has been completed [17, 18, 19, 20, 21], and an analogue of GLAP equation relevant to describe Q^2 evolution of the whole x dependent distributions has also been derived in [18, 21]. These equations for the twist-3 distributions are the evolution equation for the corresponding parent distributions and is not convenient for practical applications. However, there is a very useful news for physicists working on higher twist effects. It has been proved that at large N_c , the Q^2 evolution of all the twist-3 distributions is described by simple GLAP equations with slightly different forms for the anomalous dimensions from the twist-2 distributions [22, 23, 20]:¹ The Q^2 evolution (for g_2 , only for nonsinglet piece) is given by

$$\mathcal{M}_n [\tilde{g}_2(Q^2)] = L^{\gamma_n^g/b_0} \mathcal{M}_n [\tilde{g}_2(\mu^2)], \quad (3)$$

$$\mathcal{M}_n [\tilde{h}_L(Q^2)] = L^{\gamma_n^h/b_0} \mathcal{M}_n [\tilde{h}_L(\mu^2)], \quad (4)$$

$$\mathcal{M}_n [e(Q^2)] = L^{\gamma_n^e/b_0} \mathcal{M}_n [e(\mu^2)], \quad (5)$$

where $\mathcal{M}_n[g(Q^2)] \equiv \int_{-1}^1 dx x^n g(x, Q^2)$, $L \equiv \alpha_s(Q^2)/\alpha_s(\mu^2)$, $b_0 = \frac{11}{3}N_c - \frac{2}{3}N_f$. \tilde{g}_2 and \tilde{h}_L denote the twist-3 parts of g_2 and h_L , respectively. The corresponding anomalous dimensions in (3)- (5) are given by

$$\gamma_n^g = 2N_c \left(S_n - \frac{1}{4} + \frac{1}{2(n+1)} \right), \quad (6)$$

$$\gamma_n^h = 2N_c \left(S_n - \frac{1}{4} + \frac{3}{2(n+1)} \right), \quad (7)$$

$$\gamma_n^e = 2N_c \left(S_n - \frac{1}{4} - \frac{1}{2(n+1)} \right), \quad (8)$$

with $S_n = \sum_{j=1}^n \frac{1}{j}$. Furthermore, these anomalous dimensions are the lowest eigenvalues of the anomalous dimension matrices at large N_c . Since these relations are obtained by a mere replacement $C_F = (N_c^2 - 1)/2N_c \rightarrow N_c/2$ in the complete one-loop anomalous dimension

¹ In a recent work [24], it has also been shown that the same simplification at large N_c occurs for the Q^2 dependence of all the twist-3 fragmentation functions.

matrices at finite N_c , the correction due to the finite value of N_c is $O(1/N_c^2) \sim 10\%$ level, which is sufficient for practical application. The essential ingredient in (3)-(8) is that a knowledge on $g_2(x)$, $h_L(x)$ and $e(x)$ at one scale is sufficient to predict them at an arbitrary scale, which is not the case at finite N_c . This fact provides us with a useful framework to confront experimental data at various Q^2 of the twist-3 distribution. In fact (3) and (6) were used to predict the shape of g_2 at high Q^2 starting from the bag model calculation [9]. A more favorable feature of h_L compared with g_2 is that h_L does not mix with gluon distributions owing to its chiral-odd nature. Therefore Q^2 evolution for h_L and e is given by (4), (5), (7) and (8) even for the flavor singlet piece and thus we can get more reliable and accurate form in the small x region compared to g_2 . This work is devoted to the study of Q^2 evolution of h_L with (4) and (7).

In the rest frame of the nucleon, one can conveniently calculate the above distributions using the MIT bag model. The result for h_1 and h_L with one quark flavor in the nucleon is given as [3]

$$h_1(x) = \frac{\omega MR}{2\pi(\omega-1)j_0^2(\omega)} \int_{|y_{min}|}^{\infty} y dy \left[t_0(\omega, y)^2 + 2t_0(\omega, y)t_1(\omega, y)\frac{y_{min}}{y} + t_1(\omega, y)^2 \left(\frac{y_{min}}{y}\right)^2 \right], \quad (9)$$

$$h_L(x) = \frac{\omega MR}{2\pi(\omega-1)j_0^2(\omega)} \int_{|y_{min}|}^{\infty} y dy \left[t_0(\omega, y)^2 - t_1(\omega, y)^2 \left(2\left(\frac{y_{min}}{y}\right)^2 - 1\right) \right]. \quad (10)$$

Here t_l is given by

$$t_l(\omega, y) = \int_0^1 dz z^2 j_l(\omega z) j_l(yz), \quad (11)$$

where j_l is the l -th order spherical Bessel function, and ω is determined by the relation $\tan \omega = -\omega/(\omega-1)$. For the lowest energy mode, $\omega = 2.04$. y_{min} is defined as $y_{min} = MRx - \omega$ with the bag radius R determined by the relation $MR = 4\omega$. h_L is decomposed into the twist-2 piece which can be expressed in terms of h_1 and a purely twist-3 piece \tilde{h}_L as

$$h_L(x) = \begin{cases} 2x \int_x^1 dy \frac{h_1(y)}{y^2} + \tilde{h}_L(x), & 0 < x < 1 \\ -2x \int_{-1}^x dy \frac{h_1(y)}{y^2} + \tilde{h}_L(x). & -1 < x < 0 \end{cases} \quad (12)$$

The bag model prediction above has to be regarded as a distribution at some low energy scale $Q^2 = \mu_{bag}^2 \leq 1 \text{ GeV}^2$. For h_1 , we regard (9) as a valence distribution at this low energy scale.

In order to evolve the bag model prediction for h_L from μ_{bag}^2 to Q^2 according to (4), we used a method in [25]. For the moment, we symbolically represent $h_{1,L}(x)$ by $h(x)$. If one defines $h_{\pm}(x) = h(x) \pm h(-x) = h(x) \mp \bar{h}(x)$, the even (odd) moments of $h_+(x)$ ($h_-(x)$) on the interval $[0, 1]$ agree with $\mathcal{M}_n[h]$, whose Q^2 evolution is given by (4) and (7) and its analogue. We assume Q^2 evolution of all the moments of $h_+(x)$ and $h_-(x)$ on $[0, 1]$ is described by the same anomalous dimensions as was often assumed to describe Q^2 evolution of $f_1(x, Q^2)$

and $g_1(x, Q^2)$, and construct $h(x, Q^2)$ on $[-1, 1]$. This is equivalent to assume that the Q^2 dependence of the moments of $h(x, Q^2)$ on $[0, 1]$ and $[-1, 0]$ are separately governed by the same anomalous dimension in (7), which is a sufficient condition to satisfy (4). To describe the method in [25], we introduce Bernstein polynomial defined by

$$b^{(N,k)}(x) = (N+1) \binom{n}{k} x^k (1-x)^{N-k} = \frac{(N+1)!}{k!} \sum_{l=0}^{N-k} \frac{(-1)^l x^{k+l}}{l!(N-k-l)!}, \quad (13)$$

and note that it satisfies the relation

$$\lim_{\substack{N, k \rightarrow \infty \\ k/N \rightarrow x}} b^{(N,k)}(y) = \delta(x-y) \quad (14)$$

for $0 < x, y < 1$. Using (14), (4) and (7), we get

$$\begin{aligned} \tilde{h}_L(x, Q^2) &= \lim_{\substack{N, k \rightarrow \infty \\ k/N \rightarrow x}} \frac{(N+1)!}{k!} \sum_{l=0}^{N-k} \frac{(-1)^l}{l!(N-k-l)!} \int_0^1 dy y^{k+l} \tilde{h}_L(y, Q^2) \\ &= \lim_{\substack{N, k \rightarrow \infty \\ k/N \rightarrow x}} \frac{(N+1)!}{k!} \sum_{l=0}^{N-k} \frac{(-1)^l}{l!(N-k-l)!} L^{\gamma_{k+l}^h/b_0} \int_0^1 dy y^{k+l} \tilde{h}_L(y, \mu^2). \end{aligned} \quad (15)$$

Since the summation over l in (15) oscillates due to the factor $(-1)^l$, the direct use of (15) is not convenient. To avoid this difficulty we shall utilize the following procedure. Expand $L^{\gamma_n^h/b_0}$ as

$$L^{\gamma_n^h/b_0} = a(L) \sum_{i=0} \frac{C_i(L)}{(n+p)^{i+\rho(L)}}, \quad (16)$$

where $a(L)$, $C_i(L)$ and p are the constants determined below. Then (15) is rewritten as

$$\begin{aligned} h(x, Q^2) &= \int_x^1 \frac{dy}{y} b(x, y; Q, \mu) h(y, \mu), \\ b(x, y; Q, \mu) &\equiv a(L) \left(\frac{x}{y}\right)^{p-1} \sum_{i=0} \left(\ln \frac{y}{x}\right)^{i+\rho-1} \frac{C_i}{\Gamma(i+\rho)}, \end{aligned} \quad (17)$$

where we have used the relation

$$\lim_{\substack{N, k \rightarrow \infty \\ k/N \rightarrow x}} \frac{(N+1)!}{k!} \sum_{l=0}^{N-k} \frac{(-1)^l}{l!(N-k-l)!} \frac{y^{k+l}}{(k+l+p)^{i+\rho}} = \frac{\theta(y-x)}{\Gamma(i+\rho)y} \left(\frac{x}{y}\right)^{p-1} \left(\ln \frac{y}{x}\right)^{i+\rho-1}. \quad (18)$$

The expansion (16) can be obtained by applying the following asymptotic expansion to γ_n^h in (7):

$$S_{n+1} \sim \gamma_E + \ln(n+1) + \frac{1}{2(n+1)} - \sum_{k=1}^{\infty} \frac{B_{2k}}{2k(n+1)^{2k}} \quad (19)$$

where $\gamma_E = 0.577\dots$ is the Euler constant and B_{2k} 's are the Bernoulli numbers. This procedure gives $p = 1$ and the coefficients C_i in (16). (See [25, 13] for the details.) We have used first four terms (i.e. up to B_8) in the expansion (19), which gives enough precision.

Next we need to determine the bag scale μ_{bag} . Phenomenological values for μ_{bag}^2 adopted in the previous studies scatters below 1 GeV^2 : Jaffe and Ross [26] extracted $\mu_{bag}^2 = 0.75 \text{ GeV}^2$ from the 5-th moment of a F_3 data. Schreiber *et al.* [13] took $\mu_{bag}^2 = 0.25 \text{ GeV}^2$ to reproduce approximate shape of F_2 at $Q^2 = 10 \text{ GeV}^2$. More recently, Stratmann determined $\mu_{bag}^2 = 0.081 \text{ GeV}^2$ by comparing the second moment (momentum sum rule) of the bag model prediction with that of the valence distribution determined by Glück *et al.* [6].² Our purpose here is to see how h_L evolves compared with other distributions such as h_1 and g_2 , and therefore we shall show the results for two values of μ_{bag}^2 , $\mu_{bag}^2 = 0.081, 0.25 \text{ GeV}^2$, for future references. For other parameters, we set $N_f = 3$, $\Lambda_{\text{QCD}} = 0.232 \text{ GeV}$ in $\alpha_s(Q^2)$.

Figure 1 (a) and (b) show the results for $xh_1(x, Q^2)$ and $xg_1(x, Q^2)$ at $Q^2 = 10 \text{ GeV}^2$ with two values of μ_{bag}^2 together with the bag calculations. For the Q^2 evolution, we have used the anomalous dimension for h_1 calculated in [27, 19]. $g_1(x, Q^2)$ at $Q^2 = 10 \text{ GeV}^2$ is strongly peaked in the small x region, since the anomalous dimension for $\mathcal{M}_0[g_1]$ is zero while it is $4/3$ for $\mathcal{M}_0[h_1]$. (If one plots h_1 and g_1 instead of xh_1 and xg_1 , this feature is more conspicuous.) Figure 2 shows the bag calculation for h_L decomposed into the twist-2 and -3 contributions [3] ((a)) and h_L evolved to $Q^2 = 10 \text{ GeV}^2$ with $\mu_{bag}^2 = 0.081 \text{ GeV}^2$ ((b)) and $\mu_{bag}^2 = 0.25 \text{ GeV}^2$ ((c)). In Fig. 3, we plot only the twist-3 piece of h_L , \tilde{h}_L , taken from Fig. 2 to see how it evolves with Q^2 . These graphs show clearly that at higher Q^2 the contribution from $\tilde{h}_L(x, Q^2)$ is significantly reduced and $h_L(x, Q^2)$ is dominated by the twist-2 contribution. Although our calculation starts from the bag model prediction, this tendency can be taken as model independent. Comparison of Fig. 3 and Fig. 1 shows that \tilde{h}_L evolves faster than h_1 as is expected from the magnitudes of the anomalous dimensions [19]. For comparison we have also shown $g_2(x, Q^2)$ in Fig. 4. Since this distribution is accessible in the polarized DIS, we plotted the combination $g_2(x, Q^2) + \bar{g}_2(x, Q^2) = g_2(x, Q^2) + g_2(-x, Q^2)$ for one quark-flavor with unit charge. At the bag scale, twist-3 contribution \tilde{g}_2 is comparable to the twist-2 contribution as in the case of h_L . This feature more or less survives even at $Q^2 = 10 \text{ GeV}^2$ in contrast to the h_L case. This is because $\gamma_n^h > \gamma_n^g$ especially at small n and hence Q^2 evolution of \tilde{h}_L in the small x region is faster than that of \tilde{g}_2 . As was stated before, flavor-singlet part of g_2 mixes with the gluon distribution and Q^2 evolution of singlet \tilde{g}_2 is not given by (3). Singlet \tilde{g}_2 is probably more enhanced at small x region. If the bag model gives a good description even for the twist-3 distribution h_L , our present study indicates that it will be extremely difficult to extract $\tilde{h}_L(x, Q^2)$ at high Q^2 . On the other hand, if future experiments show $\tilde{h}_L(x, Q^2)$ is still sizable at high Q^2 , it means that the naive bag model calculation is not suitable to describe quark-gluon correlation represented by h_L in the nucleon. In any case, it is very interesting to confirm these general features in the future collider experiments.

²Comparison with other parton distributions in [6] gives almost the same numbers for μ_{bag} .

References

- [1] EMC collaboration, J. Ashman *et al.*, Phys. Lett. **B206** (1988) 364.
- [2] SMC collaboration, D. Adams *et al.*, Phys. Lett. **B329** (1994) 399; **B357** (1995) 248; E143 collaboration, K. Abe *et al.*, Phys. Rev. Lett. **74** (1995) 346; **75** (1995) 25; Phys. Lett. **B364** (1995) 61.
- [3] R.L. Jaffe and X. Ji, Nucl. Phys. **B375** (1992) 527.
- [4] R.L. Jaffe, Comm. Nucl. Part. Phys. **19** (1990) 239.
- [5] E143 collaboration, K. Abe *et al.*, Phys. Rev. Lett. **76** (1996) 587.
- [6] M. Glück, E. Reya and A. Vogt, Z. Phys. **C53** (1992) 127; A.D. Martin, W.J. Stirling and R.G. Roberts, Phys. Lett. **B354** (1995) 155; H.L. Lai, *et. al.* Phys. Rev. **D51** (1995) 4763.
- [7] M. Glück, E. Reya, M. Stratmann and W. Vogelsang, Phys. Rev. **D53** (1996) 4775; T. Gehrmann and W.J. Stirling, Phys. Rev. **D53** (1996) 6100; G. Altarelli, R. Ball, S. Forte and G. Ridolfi, hep-ph/9701289.
- [8] R.L. Jaffe and X. Ji, Phys. Rev. **D43** (1991) 724.
- [9] M. Stratmann, Z. Phys. **C60** (1993) 763.
- [10] A. Chodos *et al.*, Phys. Rev. **D9** (1974) 3471.
- [11] R.L. Jaffe, Phys. Rev. **D11** (1975) 1953.
- [12] C.J. Benesh and G. Miller, Phys. Rev. **D36** (1987) 1344; **D38** (1988) 48.
- [13] A.W. Schreiber, A.W. Thomas and J.J. Londergan, Phys. Rev. **D42** (1990) 2226.
- [14] A.W. Schreiber, A.I. Signal and A.W. Thomas, Phys. Rev. **D44** (1991) 2653.
- [15] R.L. Jaffe, Nucl. Phys. **B229** (1983) 205.
- [16] V.N. Gribov and L.N. Lipatov, Sov. J. Nucl. Phys. **15** (1972) 438; L.N. Lipatov, *ibid.* **20** (1975) 94; G. Altarelli and G. Parisi, Nucl. Phys. **B126** (1977) 298.
- [17] E.V. Shuryak and A.I. Vainshtein, Nucl. Phys. **B201** (1982) 141; P.G. Ratcliffe, Nucl. Phys. **B264** (1986) 493; I.I. Balitsky and V.M. Braun, Nucl. Phys. **B311** (1988/89) 541; X. Ji and C. Chou, Phys. Rev. **D42** (1990) 3637; J. Kodaira, Y. Yasui and T. Uematsu, Phys. Lett. **B344** (1995) 348; J. Kodaira, Y. Yasui, K. Tanaka and T. Uematsu, Phys. Lett. **B387** (1996) 855.
- [18] A.P. Bukhvostov, E.A. Kuraev and L.N. Lipatov, Sov. Phys. JETP **60** (1984) 22.
- [19] Y. Koike and K. Tanaka, Phys. Rev. **D51** (1995) 6125.
- [20] Y. Koike and N. Nishiyama, Phys. Rev. **D55** (1997) 3068.
- [21] A.V. Belitsky and D. Müller, hep-ph/9702354.
- [22] A. Ali, V.M. Braun and G. Hiller, Phys. Lett. **B266** (1991) 117.
- [23] I.I. Balitsky, V.M. Braun, Y. Koike and K. Tanaka, Phys. Rev. Lett. **77** (1996) 3078.

- [24] A.V. Belitsky, hep-ph/9702356.
- [25] A. González-Arroyo, C. López and F. J. Ynduráin, Nucl. Phys. **B153** (1979) 161.
- [26] R.L. Jaffe and G.G. Ross, Phys. Lett. **B93** (1980) 313.
- [27] X. Artru and M. Mekhfi, Z. Phys. **C45** (1990) 669.

Figure captions

Fig. 1 (a) Bag model calculation for $xh_1(x)$ (dash-dot line) and $h_1(x, Q^2 = 10 \text{ GeV}^2)$ with $\mu_{bag}^2 = 0.081 \text{ GeV}^2$ (solid line) and 0.25 GeV^2 (dashed line). (b) The same as (a) but for for $xg_1(x, Q^2)$.

Fig. 2 (a) Bag model calculation for $h_L(x)$ (solid line) decomposed into the twist-2 (dashed line) and the twist-3 (dash-dot line) contributions. (b) $h_L(x, Q^2)$ at $Q^2 = 10 \text{ GeV}^2$ with $\mu_{bag}^2 = 0.081 \text{ GeV}^2$ decomposed into the twist-2 and twist-3 contributions. (c) The same as (b) but with $\mu_{bag}^2 = 0.25 \text{ GeV}^2$.

Fig. 3 Twist-3 contribution to $h_L(x, Q^2)$ at the bag scale (dash-dot line) and $Q^2 = 10 \text{ GeV}^2$ with $\mu_{bag}^2 = 0.081 \text{ GeV}^2$ (solid line) and 0.25 GeV^2 (dashed line).

Fig. 4 (a) Bag model calculation for $g_2(x)$ decomposed into the twist-2 ($g_2^{WW}(x)$) and the twist-3 ($\tilde{g}_2(x)$) contributions. (b) $g_2(x, Q^2)$ at $Q^2 = 10 \text{ GeV}^2$ with $\mu_{bag}^2 = 0.081 \text{ GeV}^2$. (c) The same as (b) but with $\mu_{bag}^2 = 0.25 \text{ GeV}^2$.

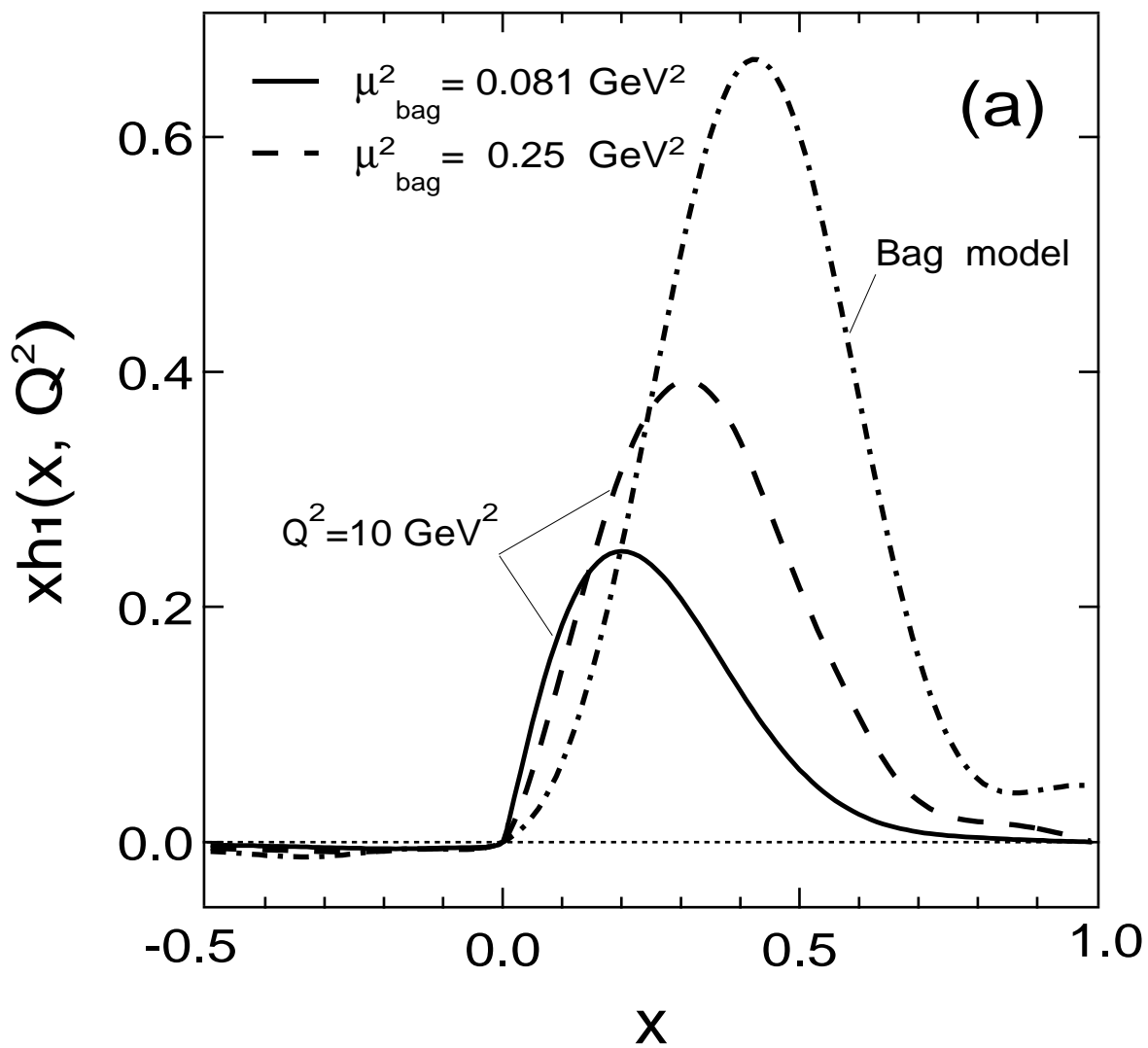


Fig.1(a)

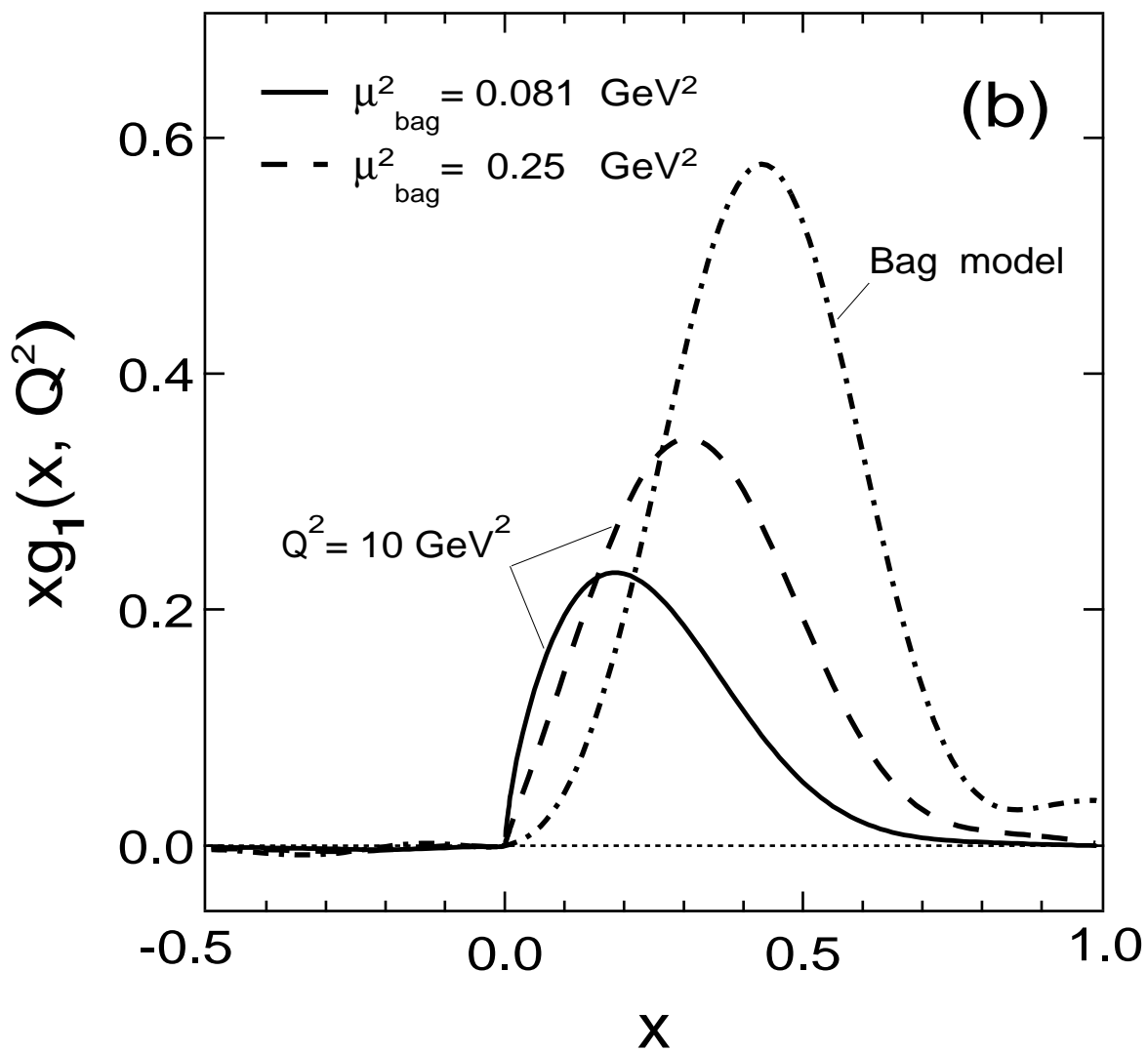


Fig.1(b)

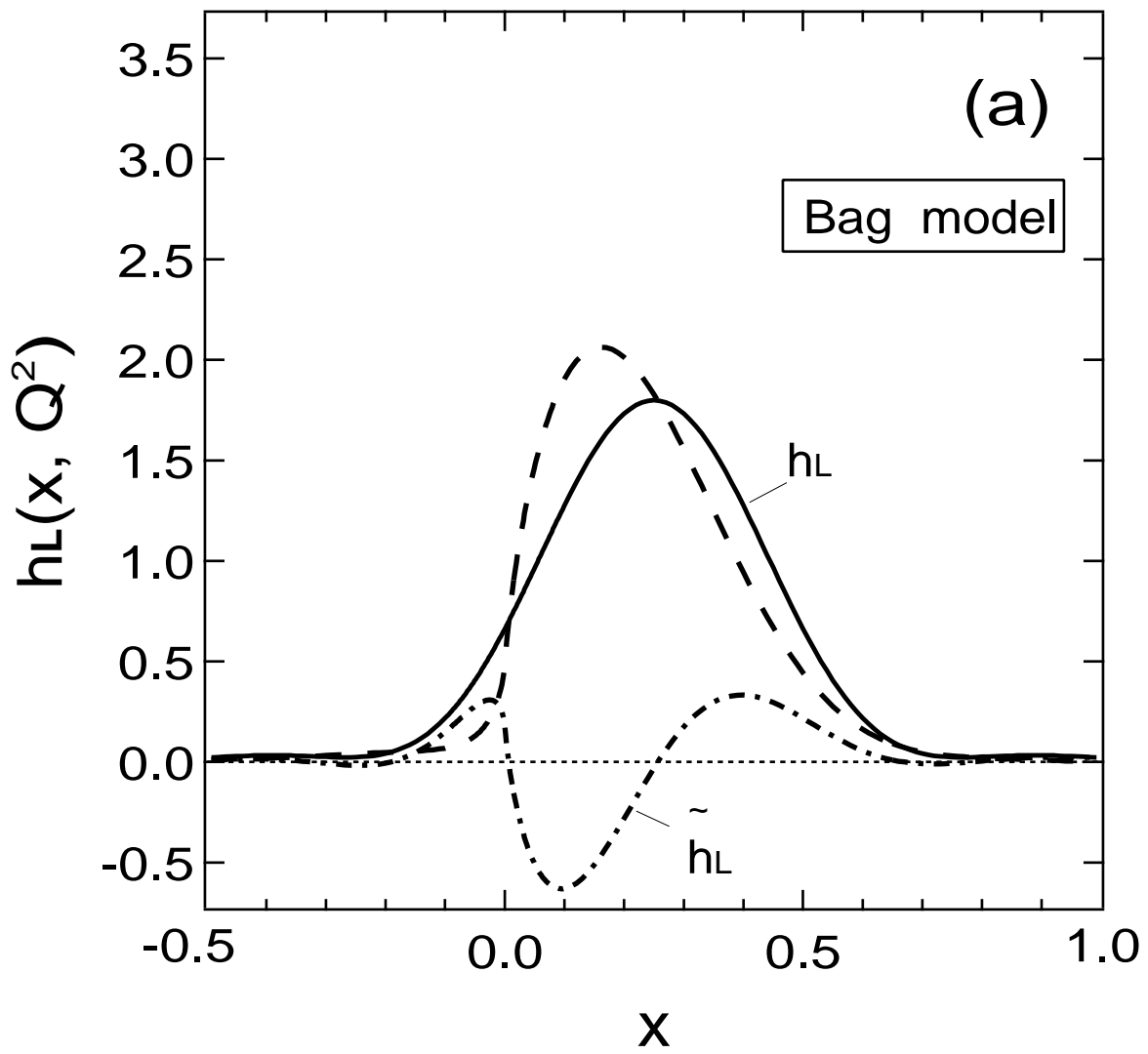


Fig.2(a)

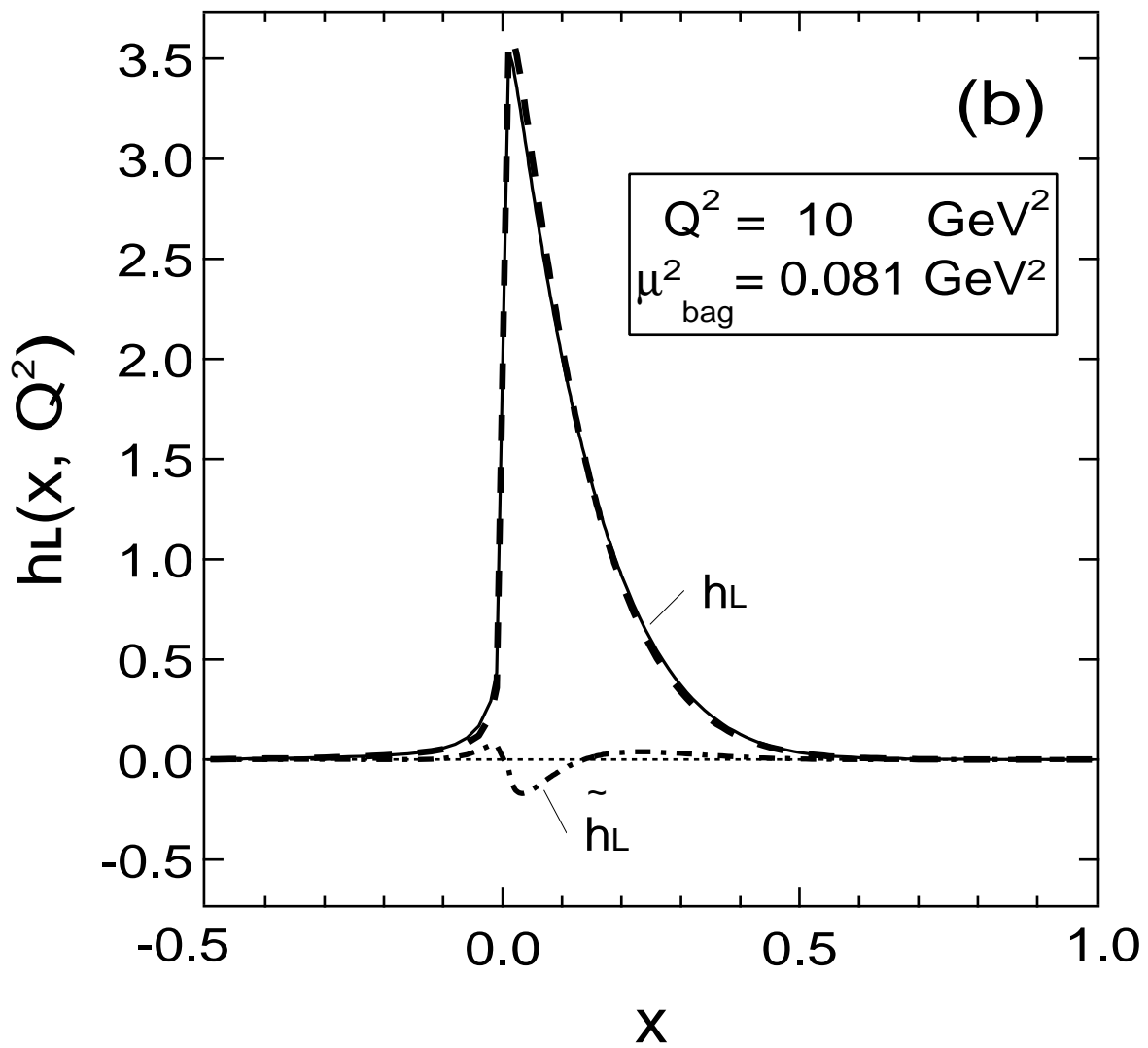


Fig.2(b)

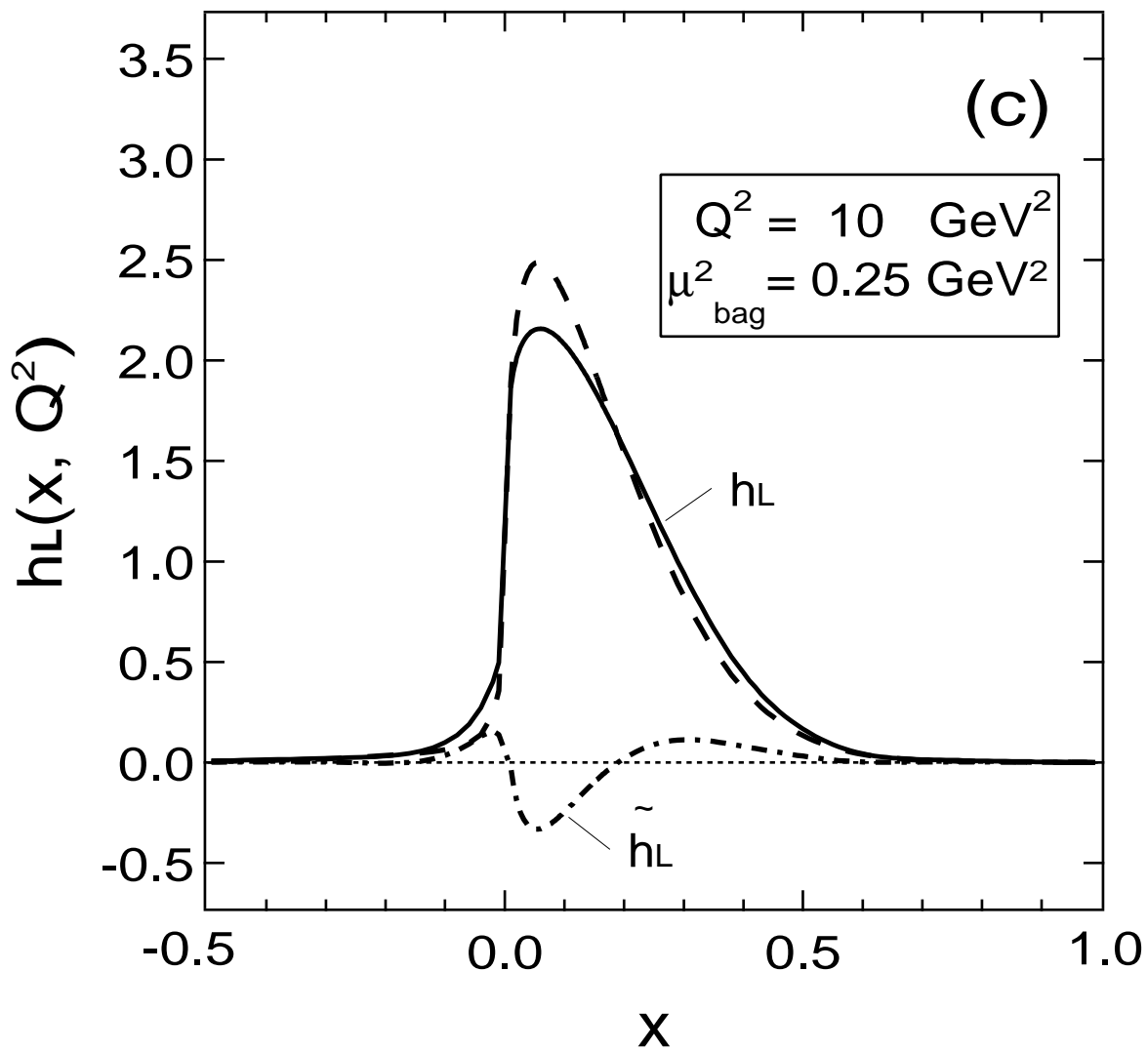


Fig.2(c)

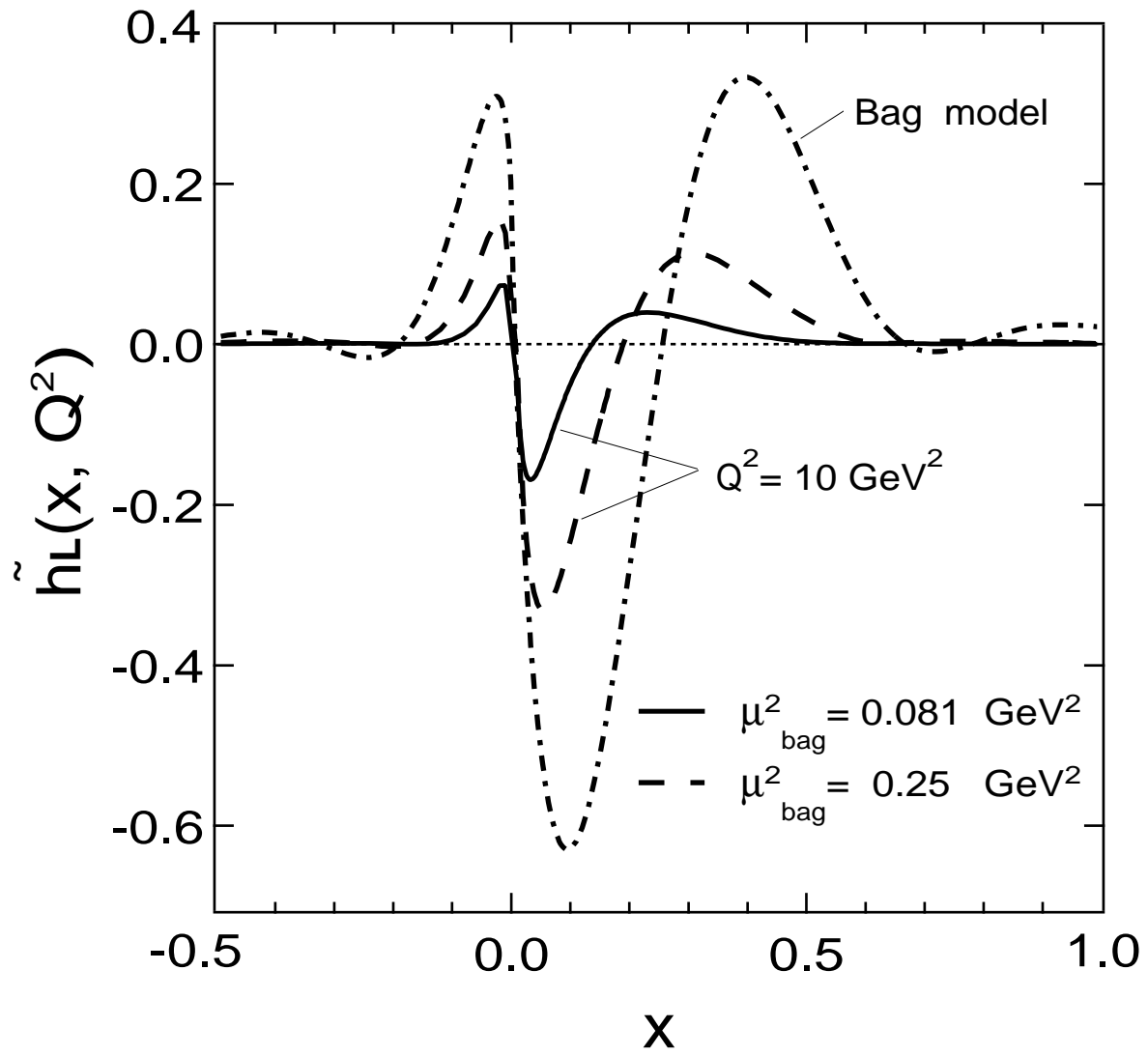


Fig.3

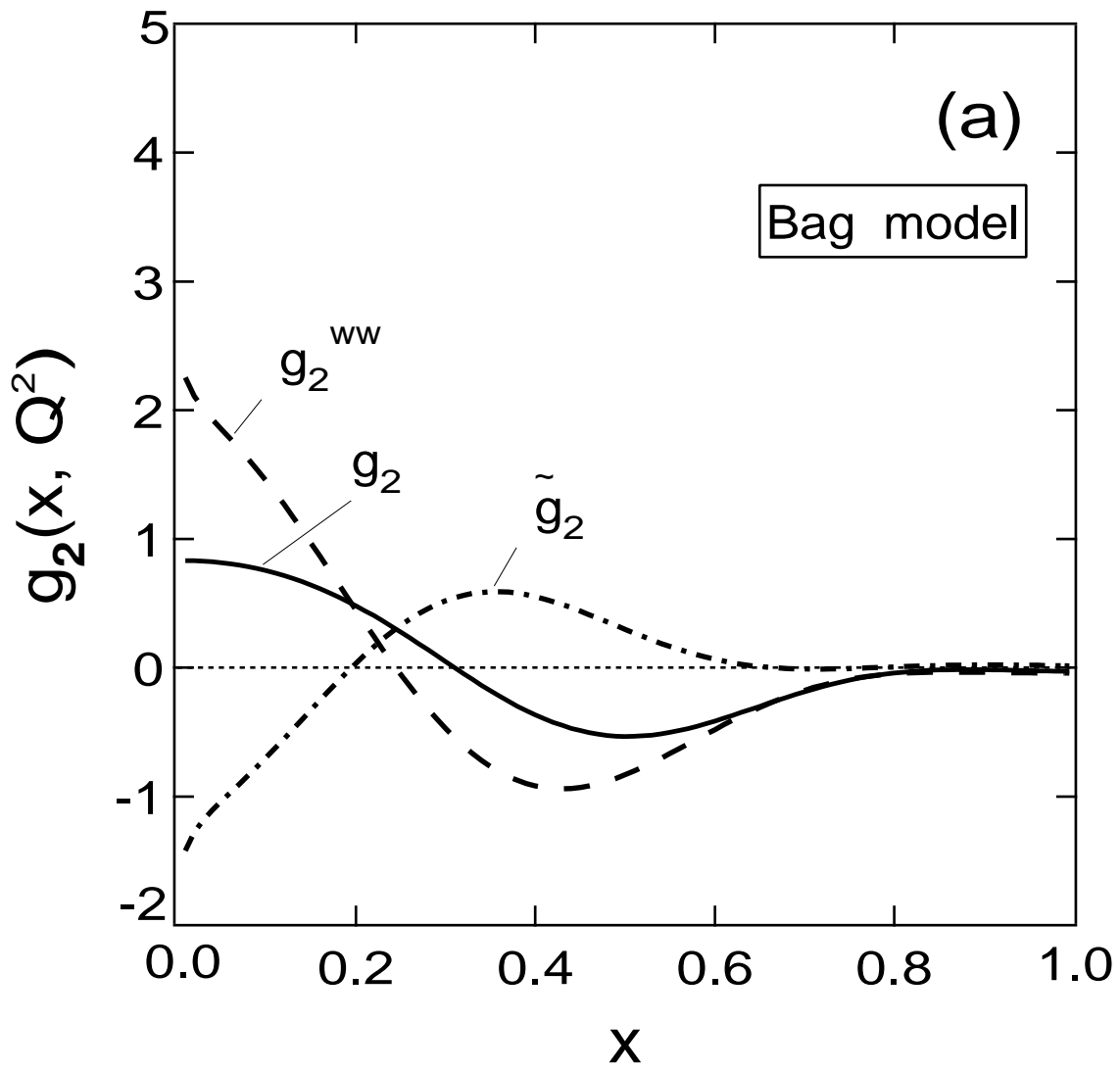


Fig.4(a)

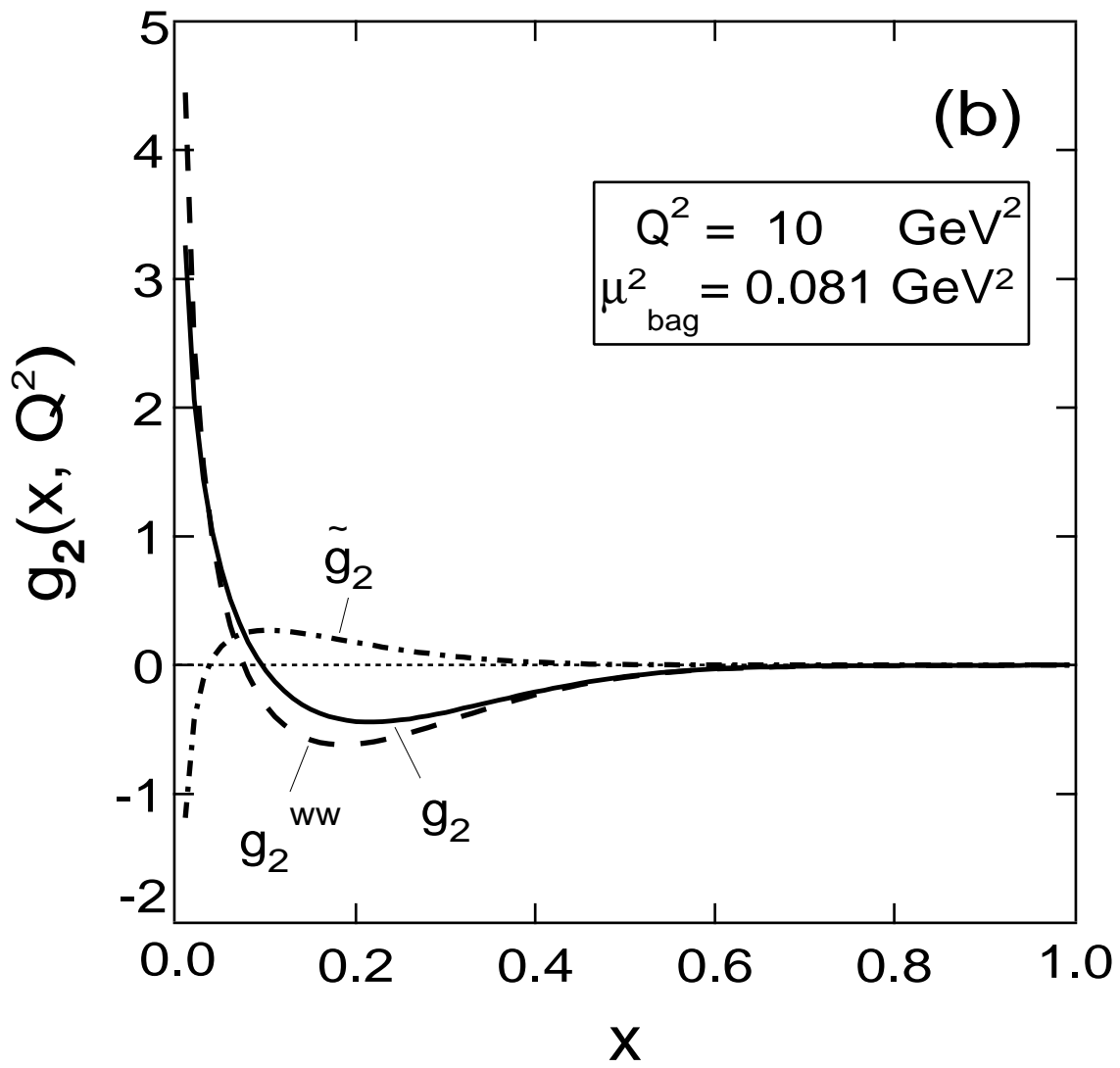


Fig.4(b)

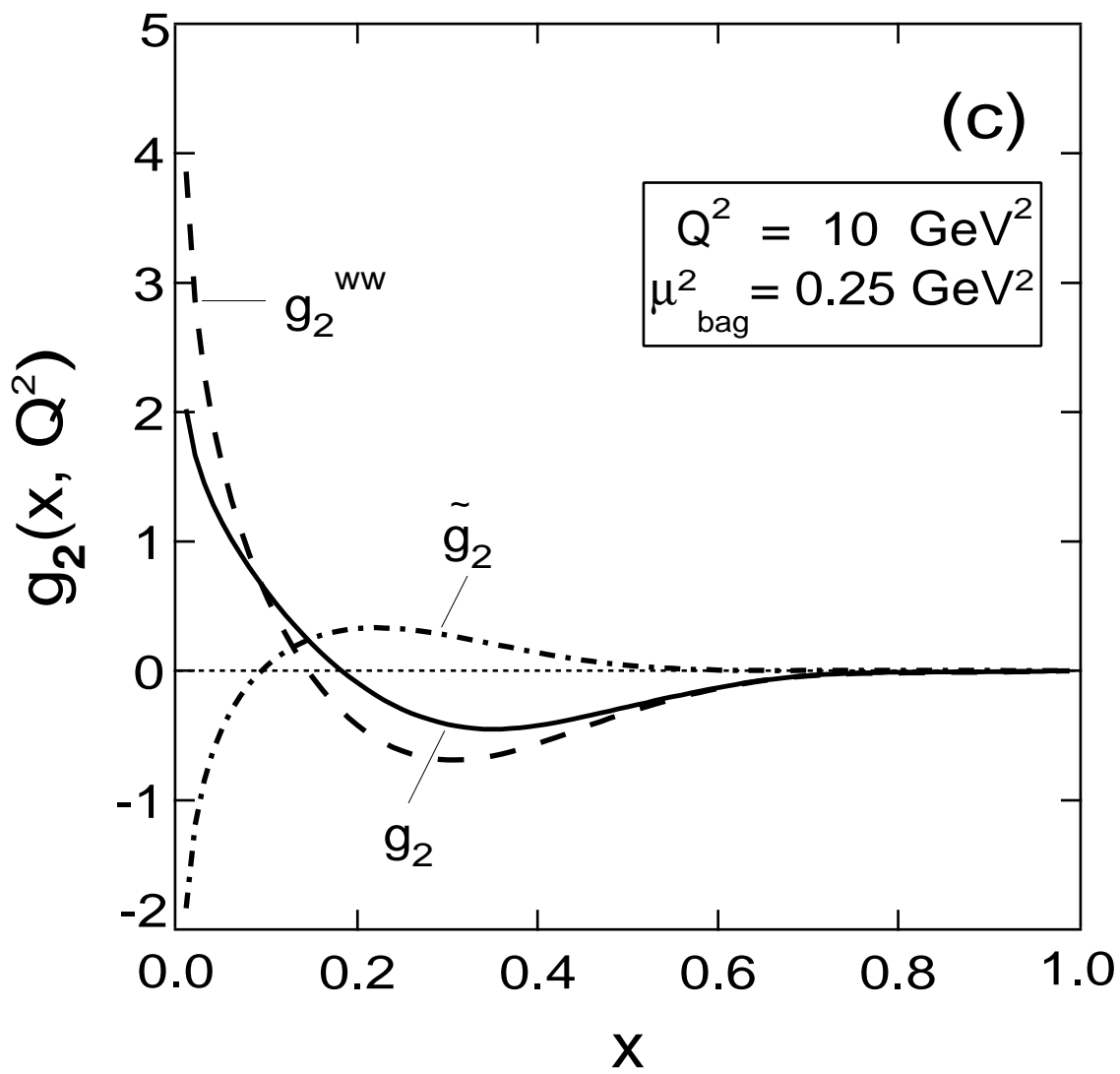


Fig.4(c)